

---

# RESEARCH ON GENDER-RELATED FINGERPRINT FEATURES


---

A PREPRINT

 **Yong Qi**<sup>\*1,2</sup>  
qiyong@sust.edu.cn

 **Yanping Li**<sup>1,2</sup>  
yanpinglics@gmail.com

 **Huawei Lin**<sup>1,2,3</sup>  
huaweilin.cs@gmail.com

 **Jiashu Chen**<sup>1,2</sup>  
gaasyu.chan@gmail.com

**Huaiguang Lei**<sup>1</sup>  
leihg@sust.edu.cn

## ABSTRACT

Fingerprint is an important biological feature of human body, which contains abundant gender information. At present, the academic research of fingerprint gender characteristics is generally at the level of understanding, while the standardization research is quite limited. In this work, we propose a more robust method, Dense Dilated Convolution ResNet (DDC-ResNet) to extract valid gender information from fingerprints. By replacing the normal convolution operations with the atrous convolution in the backbone, prior knowledge is provided to keep the edge details and the global reception field can be extended. We explored the results in 3 ways: 1) The efficiency of the DDC-ResNet. 6 typical methods of automatic feature extraction coupling with 9 mainstream classifiers are evaluated in our dataset with fair implementation details. Experimental results demonstrate that the combination of our approach outperforms other combinations in terms of average accuracy and separate-gender accuracy. It reaches 96.5% for average and 0.9752 (males) / 0.9548 (females) for separate-gender accuracy. 2) The effect of fingers. It is found that the best performance of classifying gender with separate fingers is achieved by the right ring finger. 3) The effect of specific features. Based on the observations of the concentrations of fingerprints visualized by our approach, it can be inferred that loops and whorls (level 1), bifurcations (level 2), as well as line shapes (level 3) are connected with gender. Finally, we will open source the dataset that contains 6000 fingerprint images.

**Keywords** Fingerprint · Gender Identifications · Finger Contribution · Feature Visualization

## 1 Introduction

Fingerprint gender identification aims to extract gender-related features from an unidentified fingerprint to recognize one's gender information. It can be divided into two stages, namely extracting as well as classifying Abdullah et al. [2016a,b], Gnanasivam and Muttan [2012], Gupta and Rao [2014], Mishra and Maheshwary [2017], Rekha et al. [2019], Shinde and Annadate [2015], Wedpathak et al. [2018], in which the former step is of great significance since the effectiveness of gender identification, is primarily determined by the sufficiency of gender-related features. Nowadays, Fingerprints can be classified into three level Karu and Jain [1996] Henry [1913] as shown Figure 1. Classifying ridge-related features extracted manually has achieved fairly good results, reaching an overall accuracy for 90% for average Arun and Sarath [2011], Badawi et al. [2006], Wedpathak et al. [2018]. High performances, however, depends strongly on the manual extraction of features from well-selected regions Kralik and Novotny [2003]. These methods have major shortcomings, such as high error, weak robustness, and high labor consumption. So far, with the growing popularity of machine learning and deep learning, automatic feature extraction has become a major focus.

---

\*Corresponding Author

1. School of Electronic Information & Artificial Intelligence, Shaanxi University of Science & Technology, Xi'an 710021, China  
 2. Shaanxi Joint Laboratory of Artificial Intelligence (Shaanxi University of Science & Technology), Xi'an 710021, China  
 3. College of Computer Science and Software Engineering, Shenzhen University, Shenzhen 518060, China

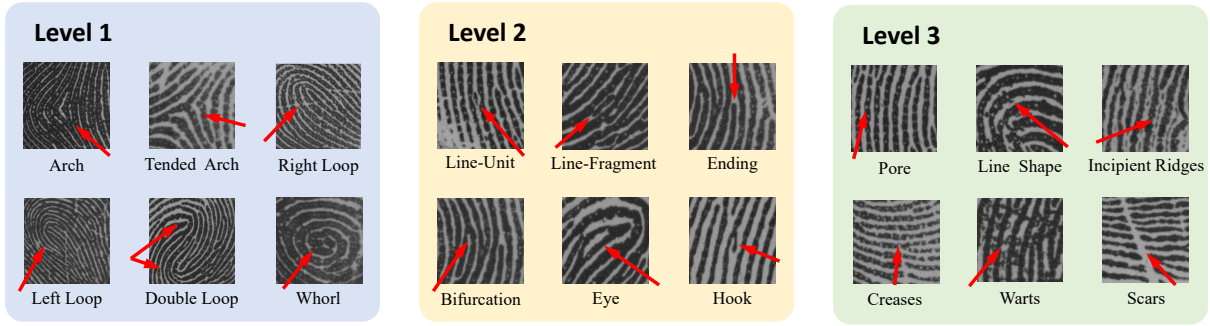


Figure 1: Three levels of fingerprints

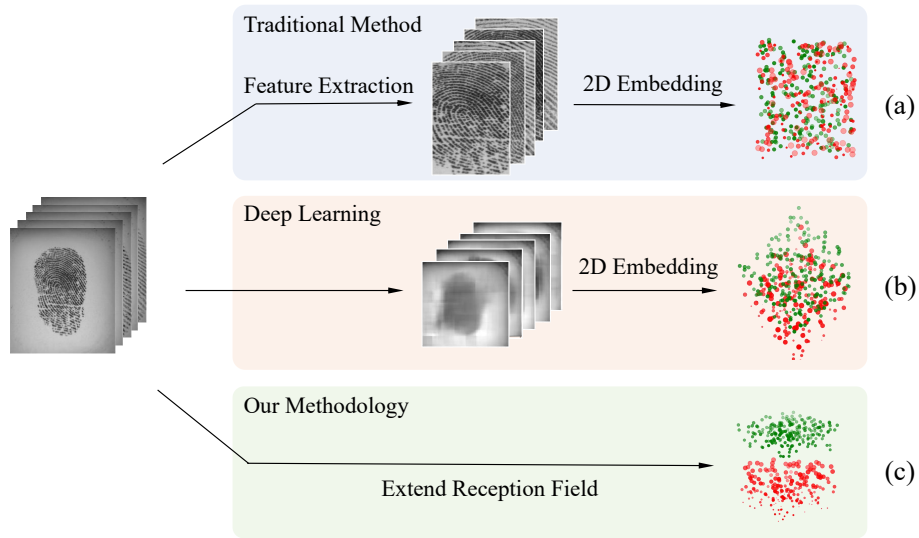


Figure 2: General automatic gender classification methods preview. (a) shows embedding and feature extracted by traditional method, which are difficult to distinguish; (b) shows deep learning method, and it is easier to identify than (a); and (c) is the result of our experiment and it performs best.

To realize the automatic feature extraction, considerable work has been done. In machine learning, methods such as DWT, SVD, PCA as well as FFT are extensively used Gnanasivam and Muttan [2012], Kaur and Mazumdar [2012], Marasco et al. [2014]. For deep learning based methods, including deep autoencoder neural networks such as VGG and ResNet, etc have been investigated Chen et al. [2017].

Although numerous algorithms have been proposed, there are still 2 major challenges. First, traditional approaches acquire excessive labor consumption and lack automation. Second, the automatic feature extraction method lacks robustness, which only concerns regions instead of considering the global field. Figure 2 shows the difference between the normal automatic feature extraction method and the deep neural network with global reception consideration. The latter can divide the feature space normatively. Besides, private datasets with disparate data distributions and sizes will directly influence the accuracy. Thus, because of the above challenges, we propose a global feature extraction method to improve the efficiency of gender classification.

### Contributions of this paper:

1. We propose a feature extraction method of fingerprint that takes global features into account. For existing typical automatic feature extraction methods and classification methods, we make comprehensive comparisons with fair implementation details.
2. We make a comprehensive comparison to test the efficiency of our method. The finger with the richest gender-related features is detected using the highest performance method. Finally, we visualize the concentrations using the selected method, which indicates the regions with the highest contributions and their corresponding specific features in the gender identification task.
3. We will finally open source the dataset since the open-source datasets in fingerprint gender classification are limited.

The following article will be divided into 4 parts. Part 2 summarizes the development over the last few years. The introduction to automatic feature extraction and classification methods used in this article is provided in part 3. All results and discussions can be found in part 4. At last, we will conclude and outlook future work.

## 2 Related Work

Previous discussions have demonstrated that gender-related features have a significant impact on fingerprint gender identification. In this section, we will first go through the evolution and then review the progress in recent years in a conclusive table, which is shown in Table 1.

In 1999, Acree [1999] manually counted ridges in specific areas on the fingerprint epidermis, showing that ridge count can determine the gender. Then in 2003, the mean epidermal ridge breadth has been proposed to identify gender Kralik and Novotny [2003]. Similarly in 2006, Badawi et al. [2006] manually extracted ridge counts, ridge thickness to valley thickness ratio (RTVTR), and white lines count to determine the gender using a neural network as a classifier. Later, Gungadin [2007] found a threshold of the ridge density 13ridges/25mm<sup>2</sup> in 2007, which determines the gender as male when the ridge density is lower than the threshold. In other words, the female has higher ridge density is probably due to they have lower ridge breadth Kralik and Novotny [2003].

Owing to the inevitable error and high manpower consumption of manual feature extractions, automatic fingerprint extraction has been proposed. In 2012, ridge features have been analyzed in the spatial domain using FFT, 2D-DCTT, and PSD Kaur and Mazumdar [2012], reaching an accuracy of 90% for females and 79.07% for males, respectively. In the same year, Gnanasivam and Muttan [2012] proposed a method using DWT and SVD as the feature extractor. In 2014, Marasco et al. [2014] utilized LBP and LPQ on texture features and used PCA to reduce the features, then the kNN classifier was applied to the extracted features. In 2017, DWT feature extraction was applied, matching with neural network Gupta and Rao [2014]. Since the presence of the deep convolution autoencoder neural network, deep learning has been widely applied in the feature extraction task especially in the biometric recognition field Chen et al. [2017].

## 3 Overview of Feature Extraction and Classification Algorithms

In this section, we will introduce our approaches and the implementation principles of automatic feature extraction methods. In addition, we will outline the classification methods utilized in this paper.

### 3.1 Feature Extraction

#### 3.1.1 Discrete Wavelet Transformation

Wavelet has been extensively applied in feature extraction, soft-biometrics recognition, and denoising, etc. It decomposes an image into sub-bands containing frequency and orientation information to represent the valid signals. Specifically, a fingerprint image is decomposed into 4 sub-bands at one level, namely low-low (LL), low-high (LH), high-low (HL) and high-high (HH) which is shown in Figure 3. Typically, the LL sub-band will be decomposed repeatedly since it is thought to represent the most energy, and  $k$  refers to the repeat times. If  $k$  is set,  $(3 \times k) + 1$  sub-bands are available. The energy of each sub-band is calculated by equation 1, which will be used as a feature vector for gender classification

Table 1: The overview of the previous methods.

Year	Publisher	Feature Extraction	Classifier	Results	Dataset
1999	Acree Acree [1999]	Ridge counting manually	Threshold	Female ridge density is higher	Own dataset contains 400 subjects
2003	Kralik Kralik and Novotny [2003]	Mean epidermal ridge breadth	Threshold	Ridge breadth is 9% greater in males than in females	Own dataset contains 60 subjects
2006	Badawi Badawi et al. [2006]	RTVTR, white line, ridge thickness	Neural Network	Average 88.8%	Own dataset contains 220 subjects
2007	Gungadin Sudesh Gungadin [2007]	Counting ridges in the upper portion of the radial border	Threshold	Ridge density of male's fingerprint tend to be less than or equal to 13ridges/25mm <sup>2</sup>	Own dataset contains 500 subjects
2011	Arun Arun and Sarath [2011]	Ridge count, ridge density, white line and RTVTR	SVM with RBF kernel	Overall 96%	Own dataset contains 150 male and 125 female images
2012	Kaur Kaur and Mazumdar [2012]	FFT, DCT, PSD	Threshold	90% for female & 79.07% for male	Own dataset contains 220 subjects
2012	Gnanasivam Gnanasivam and Muttan [2012]	DWT+SVD	KNN	91.67% for male & 84.69% for female	Own dataset contains 357 subjects
2014	Marasco Marasco et al. [2014]	LBP and LPQ descriptor	KNN	Overall 88.7%	Own dataset contains 494 subjects
2014	Gupta Gupta and Rao [2014]	DWT	ANN	Overall 91.45%	Own dataset contains 55 subjects
2016	Abdullah Abdullah et al. [2016a]	Ridge count, ridge density, white line and RTVTR	J48	Overall 96.28%	Own dataset contains 296 subjects
2016	Abdullah Abdullah et al. [2016c]	Ridge count, ridge density, white line and RTVTR	MLP	Overall 97.25%	Own dataset contains 300 subjects
2017	Sheetlani Sheetlani et al. [2017]	DWT	CNN	Overall 96.60%	Own dataset contains 80 subjects
2017	Ashish Mishra Mishra and Maheshwary [2017]	minutiae, incipient ridges	SVM & NN	76.06% for SVM and 83.7 % for female	NIST
2018	Wedpathak Wedpathak et al. [2018]	Ridge count & RTVTR	ANN	88% for male & 78% for female	Own dataset
2019	Alam Alam et al. [2019]	DWT+SVD	KNN	91.25% for male & 88.96% for female	Own dataset contains 42 subjects
2019	Rekha Rekha et al. [2019]	Gabor filter	KNN, SVM, Naive Bayes	\	\
2020	DDC-ResNet (Ours)	Autoencoder	CNN	<b>97.52%</b> for male & <b>95.48%</b> for female	Dataset contains 200 subjects

$(E_k)$ , where  $X_k(i, j)$  represents the pixel at the position  $i$  and  $j$  on the  $k$ -th level.  $W$  and  $H$  represent the width and the height of the sub-band, respectively.

$$E_k = \frac{1}{WH} \sum_{i=1}^W \sum_{j=1}^H |X_k(i, j)| \quad (1)$$

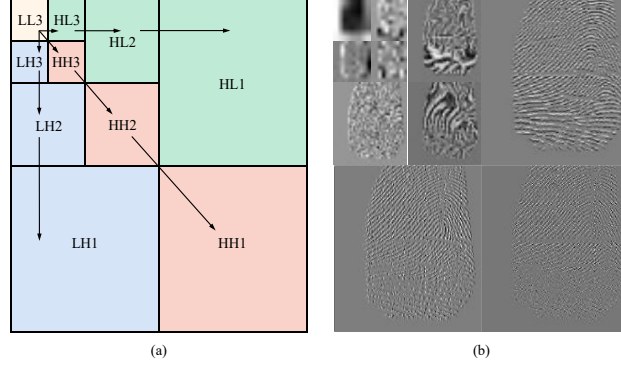


Figure 3: Discrete Wavelet Transformation (DWT). (a) Representation of level 3 DWT. (b) Fingerprint at different 3-level DWT sub-bands

### 3.1.2 Singular Value Decomposition

The fundamental of the SVD is that any rectangular matrix can be transformed into the product of three new matrices. Specifically, given a fingerprint image matrix  $A$  with  $H$  rows and  $W$  columns, it can be factored into  $U$ ,  $S$ , and  $V$  by using equation 2, where  $U = AA^T$  and  $V = A^T A$  and  $S$  are diagonal matrices that contain the square root eigenvalues with the size of  $H$  by  $W$ , which is stored for gender classification.

$$A = USV^T \quad (2)$$

### 3.1.3 Fast Fourier Transform

The FFT is used to transform a fingerprint image into the frequency domain. The transformed vector contains most of the information in the spatial domain and is used for gender classification. It is presented in equation 3, where  $M$  and  $N$  represent the height and width of the fingerprint image,  $k$  and  $l$  represent frequency variables, respectively.  $0 \leq m, k \leq M - 1, 0 \leq n, l \leq N - 1$ .

$$F[k, l] = \frac{1}{\sqrt{MN}} \sum_{n=0}^{N-1} \sum_{m=0}^{M-1} f[m, n] e^{-j2\pi(\frac{mk}{M} + \frac{nl}{N})} \quad (3)$$

### 3.1.4 Our method

Autoencoder neural networks can be divided into the encoder and decoder. Concretely, in the encoder step, the low dimensional data will be compressed into feature vector in high dimensional space, and the decoder step is to reconstructs the original data without redundant features. The general equation is described in 4. The feature vector can be optimized by minimizing the distance between the original data and the reconstructed data, and used for gender classification. Our method utilizes ResNet as the backbone, and uses the atrous convolution operation to replace the normal convolutions, as shown in Figure 4. In the block res we utilize atrous rates as 1, 2 and 5 to prevent the gridding effect.

$$y' = D(E(x), x) \quad (4)$$

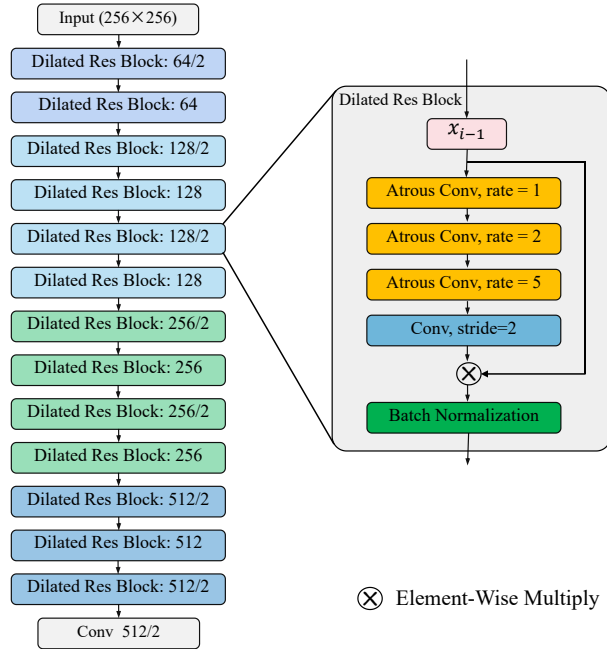


Figure 4: Architecture of DDC-ResNet for gender information extracting. The input fingerprint image is of size  $256 \times 256$ . (Right) The basic dilated residual block in the DDC-ResNet, where  $x_{i-1}$  is the feature map from previous block.

### 3.2 Gender Classification

To ensure fairness of experiments, we adopt commonly used 9 classifiers in gender classification problem, which are CNN, SVM (3 kernels), kNN, Adaboost, J48, ID3, and LDA. Among them the 3 kernels in SVM refer to linear, radial basis function, and polynomial, respectively. CNN is comprised of fully connected layers. These are all mainstream algorithms used in classification tasks. We therefore only highlight their implementation details in the next section and more details of the methods are presented in section 4.1.

## 4 Experimental Results

In this section, we first introduce our dataset and adopted implementation details. In the experimental stage, factors that affect gender-related features will be analyzed comprehensively to provide some useful conclusions.

### 4.1 Experimental Setup

#### 4.1.1 Dataset

The fingerprint dataset used in experiments is obtained from ZK fingerprint acquisition equipment with 500 dpi, containing 200 persons (102 females and 98 males) and 6000 images. Each finger is collected 3 times to guarantee the quality of the fingerprint image.

#### 4.1.2 Implementation Details

In the preprocessing step, we resize each fingerprint image to  $256 \times 256$  and normalize it to  $[0, 1]$ . *Train* : *Test* ratio is 4 : 1, No repetitive finger is guaranteed in both the training set and test set.

In the feature extraction stage, for DWT, each fingerprint goes through eight levels of decomposition. For SVD, each fingerprint image vector is of size 256. In VGG-Net, we apply the VGG-19 network in which 8 blocks are utilized. Each block contains 2 convolutional layers and a batch of normalization layers. ResNet-18 is applied and each

block contains a residual block to prevent the vanishment of gradients. The DDC-ResNet, by replacing the normal convolutional layers with dilated convolutional layers in ResNet, lowers the loss of valid edge features Wang et al. [2018]. To keep the fairness, these three types of feature extraction networks are of the vector size  $[-1, 512]$  in the last layer. Here we set the batch size to be 10, and the iteration numbers are 10K. The optimizer we adopt is Adam, in which the learning rate is  $3 \times 10^{-4}$ . Inspired by Maas Maas et al. [2013], the leaky relu is used as the activation function. All the codes are realized with the framework TensorFlow Abadi et al. [2016] in python. Hardware utilization includes GPU with NVIDIA TITAN Xp, and CPU with 2.8GHz, 32GB in RAM.

In the classification progress, the Adaboost is used with the  $n\_estimator = 100$ ,  $learning\ rate = 0.01$ ,  $max\_depth = 7$ , and  $subsample = 1.0$ . In SVM, the linear kernel is utilized with the function LinearSVC in the default configuration,  $C = 100$  and  $gamma = 0.5$  are set when applying RBF and polynomial kernels. The parameter  $k$  in kNN is set to be 1. J48 algorithm is conducted in WEKA software with the default settings Holmes et al. [1994]. The CNN classifier is comprised of 3 fully connected layers with the leaky relu activation. Classification algorithms except J48 and CNN are all conducted in scikit-learn Pedregosa et al. [2011].

Table 2: The upper value in each cell represents *average accuracy (%)*, and the under value shows separate gender accuracy, meaning *male accuracy/female accuracy*.

	Adaboost	SVM <sup>1</sup>	SVM <sup>2</sup>	SVM <sup>3</sup>	KNN	J48	CNN	ID3	LDA
<b>FFT</b>	85.280 0.8337/0.8719	65.827 0.6895/0.6270	82.604 0.7935/0.8586	87.310 0.8653/0.8809	92.202 0.9346/0.9094	73.912 0.7224/0.7558	87.220 0.8814/0.8630	78.931 0.7682/0.8104	88.498 0.9012/0.8687
<b>DWT</b>	91.494 0.9531/0.8768	70.001 0.7280/0.6720	88.275 0.9144/0.8511	88.735 0.9452/0.8295	90.460 0.9187/0.8905	90.394 0.8977/0.9102	91.360 0.9455/0.8817	90.344 0.8727/0.9342	87.192 0.8693/0.8745
<b>SVD</b>	92.096 0.9294/0.9125	66.552 0.6839/0.6471	86.506 0.7910/0.9391	91.609 0.9248/0.9074	88.230 0.8917/0.8729	76.667 0.7296/0.8037	92.413 0.9350/0.9133	89.770 0.8856/0.9098	89.721 0.9411/0.8443
<b>ResNet</b>	92.068 0.9334/0.9080	69.302 0.7202/0.6658	85.502 0.8210/0.8890	91.713 0.9220/0.9123	92.529 0.9072/0.9434	90.460 0.8979/0.9113	93.333 0.9463/0.9204	90.460 0.9149/0.8943	82.106 0.7966/0.8455
<b>VGG</b>	94.138 0.9464/0.9364	72.454 0.7208/0.7283	88.506 0.8192/0.9509	94.713 0.9590/0.9353	93.563 0.9428/0.9285	88.220 0.9195/0.8449	93.678 0.9423/0.9313	90.459 0.9099/0.8993	89.385 0.9047/0.8830
<b>DDCResNet</b>	94.253 0.9350/0.9501	73.844 0.7366/0.7403	89.576 0.8260/0.9655	<b>95.333</b> <b>0.9743/0.9324</b>	92.759 0.8865/0.9687	89.344 0.8921/0.8948	<b>96.500</b> <b>0.9752/0.9548</b>	91.494 0.9159/0.9140	93.599 0.9461/0.9259

## 4.2 Effect of Methods

To evaluate the effect of different methods on gender-related features, we make a benchmark for the combinations of 6 feature extraction methods coupling with 9 classifiers to compare their average and separate-gender accuracies, as shown in Table 2. In terms of the average accuracy, the DDC-ResNet extractor outperforms other extraction methods when matching with different classifiers. For the classifiers, the Adaboost, SVM with the polynomial kernel, and CNN are more outstanding. On the contrary, the SVM with the linear kernel seems not qualified for the extracted features with high dimensional space in the gender identification task. Regarding the separate-gender performance, most of the results show more correct predictions in males than in females, especially for DWT+SVM<sup>3</sup>. The difference is more than 10%, which is agreed with the Shinde and Annadate [2015], Gnanasivam and Vijayarajan [2019], suggesting that fingerprints of males contain richer gender-related features in some aspects. To make a more comprehensive analysis, we also evaluate the time consumption of each combination when feeding different batch sizes of data. The result is shown in Table 4. In general, deep learning extractors consume more time than machine learning, and SVD extractor consumes the least time. However, FFT behaves oppositely which is because the transformation does not reduce the feature size. In summary, the combination of DDC-ResNet and CNN outperforms other combinations, reaching an average accuracy of 96.50% and separate-gender accuracy of 0.9743/0.9324. Moreover, males contain richer gender-related features than females. After evaluating the performance of various methods with all test fingers, we will explore how specific fingers influence the gender identification results below.

### 4.3 Effect of Fingers

After studying the effect of varying methods on gender-related features, we further explore the effect of each finger. We divide the testing fingerprints into 10 sets, each set of which corresponds to a specific finger containing 660 fingerprint images. We apply the DDC-ResNet coupled with CNN (best performance method above) to test the 10 sets, as listed in Table 3. The result indicates that for each specific finger, the right ring finger (R2) shows the highest accuracy, reaching 92.455%. For 5 pairs of fingers, ring fingers outperform other pairs, reaching an accuracy of 91.413%. For the overall hand, the right hand achieves a higher accuracy than the left hand, which reaches 87.872%. To better understand the effect of fingers on gender-related features, more careful studies will be carried out in the following part.

Table 3: Estimate performance of each finger (%), in which L means left hand and R means right hand,  $F_x$  represents Finger  $x$ . The index from 1 to 5 means little finger, ring finger, middle finger index finger and thumb respectively.

L1	88.291	$F_1: 87.078$	$L_{average}: 86.418$
R1	85.864		
L2	90.371	$F_2: \mathbf{91.413}$	
R2	<b>92.455</b>		
L3	87.152	$F_3: 89.258$	
R3	91.363		
L4	82.819	$F_4: 84.637$	$R_{average}: \mathbf{87.872}$
R4	86.455		
L5	83.455	$F_5: 83.340$	
R5	83.224		

Table 4: The running time of each combination, each cell means time consumption ( $s$ ) when feeding 10/100/1000 batch size of data.

	VGG	ResNet	DDCResNet	DWT	SVD	FFT
<b>Adaboost</b>	3.213/3.959/19.677	3.776/4.213/20.581	6.456/6.86/26.100	0.184/2.652/18.693	0.165/1.786/14.445	0.130/3.994/280.162
<b>SVM<sup>1</sup></b>	3.176/3.905/16.530	3.739/4.159/17.434	6.419/6.806/22.953	0.160/2.013/15.674	0.147/1.292/13.010	0.184/3.207/48.925
<b>SVM<sup>2</sup></b>	3.176/3.905/16.960	3.739/4.159/17.864	6.419/6.806/23.383	0.143/2.412/15.108	0.153/1.292/12.967	0.029/1.688/147.075
<b>SVM<sup>3</sup></b>	3.176/3.905/16.902	3.739/4.159/17.806	6.419/6.806/23.325	0.296/1.609/16.883	<b>0.146/1.291/12.944</b>	0.028/1.665/143.031
<b>KNN</b>	3.180/3.904/16.602	3.743/4.158/17.506	6.423/6.805/23.025	0.198/1.059/18.370	0.162/1.294/12.889	0.030/1.393/89.841
<b>J48</b>	3.184/3.927/16.331	3.747/4.181/17.235	6.427/6.828/22.754	0.184/1.477/15.854	0.148/1.296/12.791	0.858/4.822/201.731
<b>CNN</b>	3.189/3.903/15.963	3.752/4.157/16.867	6.432/6.804/22.386	0.139/1.749/17.110	0.156/1.300/12.756	1.200/4.190/341.870
<b>ID3</b>	3.176/3.920/16.629	3.739/4.174/17.533	6.419/6.821/23.052	0.142/1.842/15.556	0.1467/1.291/12.897	0.062/1.756/43.519
<b>LDA</b>	3.176/3.901/16.292	3.739/4.154/17.196	6.419/6.801/22.715	0.148/1.466/16.770	0.147/1.292/12.967	0.138/2.478/41.830

### 4.4 Effect of Features

To further research on gender-related features, we apply the grad-cam Selvaraju et al. [2017] technique to visualize the heat maps, seeing which part contributes most. Specifically, based on earlier results, we visualize testing fingers by using the DDC-ResNet extractor. The overview of visualization is exhibited in Figure 5, It can be seen that concentrations are mainly on or around the center of fingerprints. Detailed observation is shown in Figure 6. The concentration covers the whorl part which belongs to the pattern features of level 1. Further observation reveals that bifurcations are gathered in concentration regions. However, we exclude the sweat pores around the bifurcations since other parts containing more remarkable sweat pores have not received attention. We also find that the concentration regions prefer to be continuous parts. Therefore, it is not hard to say that the foundation of recognition is complete ridges, which explains the reason for manual extraction of minutiae features in well-selected continuous regions.



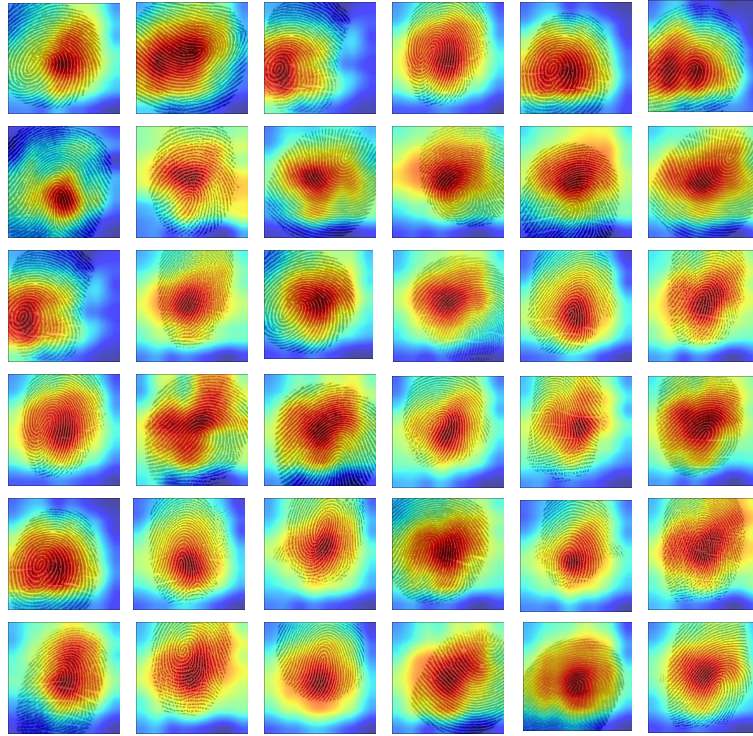


Figure 5: Grad-CAM visualizations for DDC-ResNet. The red regions in the figures correspond to high score for gender information. Best viewed in color.

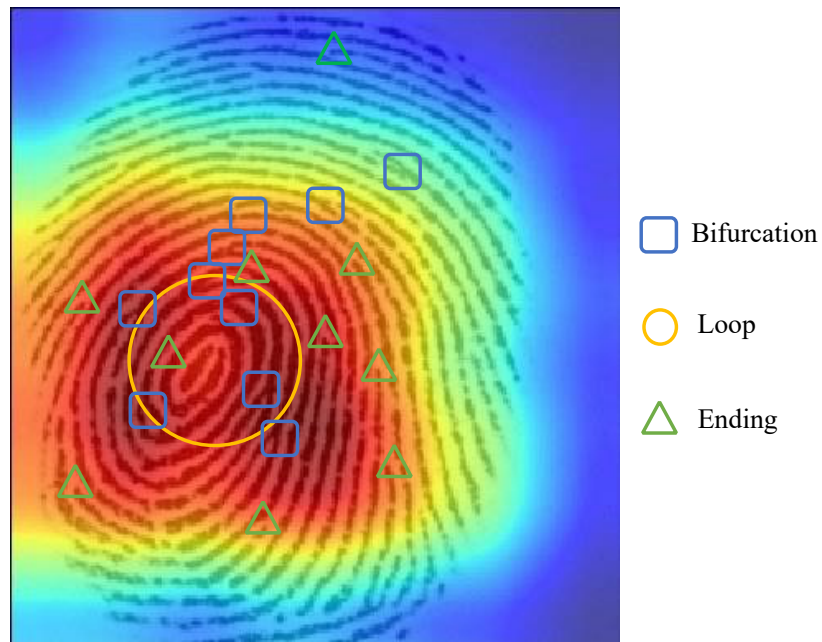


Figure 6: Visualizations of bifurcation, loop and ending in a fingerprint. The red region with more gender information in the center of the fingerprint gets higher scores.

## 5 Conclusion and Future work

This paper proposes an effective network considering the global reception field in the gender classification task, which is realized by replacing normal convolutions with dilated convolution in the extraction method. The experiment thoroughly explores the efficiency from three aspects. First, comparing our method with various methods with fair implementation details in our dataset. 6 typical automatic feature extraction methods like DWT, SVD, VGG, and our method coupling with 9 mainstream classifiers such as Adaboost, kNN, SVM, CNN, etc. are evaluated. Experimental results reveal that the combination of our extractor with the CNN classifier outperforms other combinations. For average accuracy, it reaches 96.50% and for separate-gender accuracy, it reaches 0.9752 (males) / 0.9548 (females). Second, we investigate the effect of fingers by classifying gender using separate fingers, and find the best-performing finger is the right ring finger, which reaches an accuracy of 92.455%. Third, we study the effect of features by visualizing concentrations of fingerprints. Depending on the analysis, loops/whorls (level 1), bifurcations (level 2) and line shapes (level 3) may have a close relationship with gender. This work not only comprehensively explores the efficiency of the proposed method, but also provides a way to observe fingerprint identification features much closer. These specific features will be quantified in the future to further explore the impact on fingerprint recognition.

## References

- SF Abdullah, AFNA Rahman, ZA Abas, and WHM Saad. Fingerprint gender classification using univariate decision tree (j48). *Network (MLPNN)*, 96(95.27):95–95, 2016a.
- Siti Fairuz Abdullah, AFNA Rahman, ZA Abas, and WHM Saad. Support vector machine, multilayer perceptron neural network, bayes net and k-nearest neighbor in classifying gender using fingerprint features. *International Journal of Computer Science and Information Security*, 14(7):336, 2016b.
- P Gnanasivam and Dr S Muttan. Fingerprint gender classification using wavelet transform and singular value decomposition. *arXiv preprint arXiv:1205.6745*, 2012.
- Samta Gupta and A Prabhakar Rao. Fingerprint based gender classification using discrete wavelet transform & artificial neural network. *International Journal of Computer Science and mobile computing*, 3(4):1289–1296, 2014.
- Ashish Mishra and Preeti Maheshwary. A novel technique for fingerprint classification based on naive bayes classifier and support vector machine. *International Journal of Computer Applications*, 975:8887, 2017.
- V Rekha, S Gurupriya, S Gayadhri, and S Sowmya. Dactyloscopy based gender classification using machine learning. In *2019 IEEE International Conference on System, Computation, Automation and Networking (ICSCAN)*, pages 1–5. IEEE, 2019.
- Mangesh K Shinde and SA Annadate. Analysis of fingerprint image for gender classification or identification: using wavelet transform and singular value decomposition. In *2015 International Conference on Computing Communication Control and Automation*, pages 650–654. IEEE, 2015.
- Ganesh S Wedpathak, DG Kadam, KG Kadam, AR Mhetre, and VK Jankar. Fingerprint based gender classification using ann. *International Journal of Recent Trends in Engineering & Research (IJRTER)*, 4(3):4, 2018.
- Kalle Karu and Anil K Jain. Fingerprint classification. *Pattern recognition*, 29(3):389–404, 1996.
- Edward Richard Henry. *Classification and uses of finger prints*. HM Stationery Office, printed by Darling and son, Limited, 1913.
- KS Arun and KS Sarath. A machine learning approach for fingerprint based gender identification. In *2011 IEEE Recent Advances in Intelligent Computational Systems*, pages 163–167. IEEE, 2011.
- Ahmed M Badawi, Mohamed Mahfouz, Rimon Tadross, and Richard Jantz. Fingerprint-based gender classification. *IPCV*, 6(8):1, 2006.
- Miroslav Kralik and Vladimir Novotny. Epidermal ridge breadth: an indicator of age and sex in paleodermatoglyphics. *Variability and evolution*, 11(2003):5–30, 2003.
- Ritu Kaur and Susmita Ghosh Mazumdar. Fingerprint based gender identification using frequency domain analysis. *International Journal of Advances in Engineering & Technology*, 3(1):295, 2012.
- Emanuela Marasco, Luca Lugini, and Bojan Cukic. Exploiting quality and texture features to estimate age and gender from fingerprints. In *Biometric and Surveillance Technology for Human and Activity Identification XI*, volume 9075, page 90750F. International Society for Optics and Photonics, 2014.
- Min Chen, Xiaobo Shi, Yin Zhang, Di Wu, and Mohsen Guizani. Deep features learning for medical image analysis with convolutional autoencoder neural network. *IEEE Transactions on Big Data*, 2017.

- Mark A Acree. Is there a gender difference in fingerprint ridge density? *Forensic science international*, 102(1):35–44, 1999.
- MBBS Sudesh Gungadin. Sex determination from fingerprint ridge density. *Internet Journal of Medical Update*, 2(2), 2007.
- SF Abdullah, AFNA Rahman, ZA Abas, and WHM Saad. Multilayer perceptron neural network in classifying gender using fingerprint global level features. *Indian Journal of Science and Technology*, 9(9):1–6, 2016c.
- Jitendra Sheetlani, Rajmohan Pardeshi, et al. Fingerprint based automatic human gender identification. *Int. J. Comput. Appl*, 170(7):1–4, 2017.
- Shadab Alam, Megha Dua, Ashutosh Gupta, et al. A comparative study of gender classification using fingerprints. In *2019 6th International Conference on Computing for Sustainable Global Development (INDIACom)*, pages 880–884. IEEE, 2019.
- Panqu Wang, Pengfei Chen, Ye Yuan, Ding Liu, Zehua Huang, Xiaodi Hou, and Garrison Cottrell. Understanding convolution for semantic segmentation. In *2018 IEEE winter conference on applications of computer vision (WACV)*, pages 1451–1460. IEEE, 2018.
- Andrew L Maas, Awni Y Hannun, Andrew Y Ng, et al. Rectifier nonlinearities improve neural network acoustic models. In *Proc. icml*, volume 30, page 3. Citeseer, 2013.
- Martín Abadi, Ashish Agarwal, Paul Barham, Eugene Brevdo, Zhifeng Chen, Craig Citro, Greg S Corrado, Andy Davis, Jeffrey Dean, Matthieu Devin, et al. Tensorflow: Large-scale machine learning on heterogeneous distributed systems. *arXiv preprint arXiv:1603.04467*, 2016.
- Geoffrey Holmes, Andrew Donkin, and Ian H Witten. Weka: A machine learning workbench. In *Proceedings of ANZIS'94-Australian New Zealand Intelligent Information Systems Conference*, pages 357–361. IEEE, 1994.
- Fabian Pedregosa, Gaël Varoquaux, Alexandre Gramfort, Vincent Michel, Bertrand Thirion, Olivier Grisel, Mathieu Blondel, Peter Prettenhofer, Ron Weiss, Vincent Dubourg, et al. Scikit-learn: Machine learning in python. *the Journal of machine Learning research*, 12:2825–2830, 2011.
- P Gnanasivam and R Vijayarajan. Gender classification from fingerprint ridge count and fingertip size using optimal score assignment. *Complex & Intelligent Systems*, 5(3):343–352, 2019.
- Ramprasaath R Selvaraju, Michael Cogswell, Abhishek Das, Ramakrishna Vedantam, Devi Parikh, and Dhruv Batra. Grad-cam: Visual explanations from deep networks via gradient-based localization. In *Proceedings of the IEEE international conference on computer vision*, pages 618–626, 2017.